Journal of Saudi Chemical Society (2016) **20**, 237–244

King Saud University

Journal of Saudi Chemical Society

www.ksu.edu.sa
www.sciencedirect.com

ORIGINAL ARTICLE

Hierarchically macroporous silver monoliths using Pluronic F127: Facile synthesis, characterization and its application as an efficient biomaterial for pathogens

Gowhar Ahmad Naikoo [a,c,*], Molly Thomas [a], Mohd. Anis Ganaie [b], Mehraj Ud Din Sheikh [a], Mustri Bano [a], Israr Ul Hassan [c], Farid Khan [a,*]

[a] *Nanomaterials Discovery Laboratory, Department of Chemistry, Dr. Hari Singh Gour University (A Central University), Sagar (M.P) 470003, India*
[b] *Laboratory of Flavor and Chromatographic Analysis, Federal University Sergipe, Sao Cristovao 49000-000 Brazil*
[c] *Department of Mathematics and Sciences, College of Arts and Applied Sciences, Dhofar University, Salalah, Oman*

Received 9 September 2015; revised 1 December 2015; accepted 15 December 2015
Available online 23 December 2015

KEYWORDS

Macroporous;
Biomaterials;
Pathogens;
Pluronic F127

Abstract Herein we report the facile synthesis of three dimensional macroporous (MP) silver monoliths serving as intelligent biomaterials against Gram negative (*Escherichia coli, Salmonella typhimurium*) and Gram positive (*Bacillus subtilis*) bacteria with more efficacy against Gram negative bacteria. The macroporous silver monoliths were examined by Fourier transform infra red (FTIR) spectroscopy, thermogravimetric analysis (TGA), X-ray diffraction (XRD) study, field emission scanning electron microscopy (FESEM), energy dispersion X-ray spectroscopy analysis (EDX) and Brunauer–Emmet–Teller (BET) adsorption technique. From the antibacterial activity results, it was concluded that macroporous silver monoliths can serve as efficient disinfection agents. The enhanced antibacterial properties of macroporous silver monoliths was possibly due to high surface free energy of the surface Ag^+ atoms leading to cell membrane damage followed by cell death.

* Corresponding authors at: Nanomaterials Discovery Laboratory, Department of Chemistry, Dr. Hari Singh Gour University (A Central University), Sagar (M.P) 470003, India. Tel.: +91 9425626334, +91 9009216572, +91 968 96158220.
E-mail addresses: gowhar@du.edu.om (G.A. Naikoo), faridkhan58@yahoo.com, mkzgan@yahoo.com (F. Khan).
Peer review under responsibility of King Saud University.

Production and hosting by Elsevier

http://dx.doi.org/10.1016/j.jscs.2015.12.002

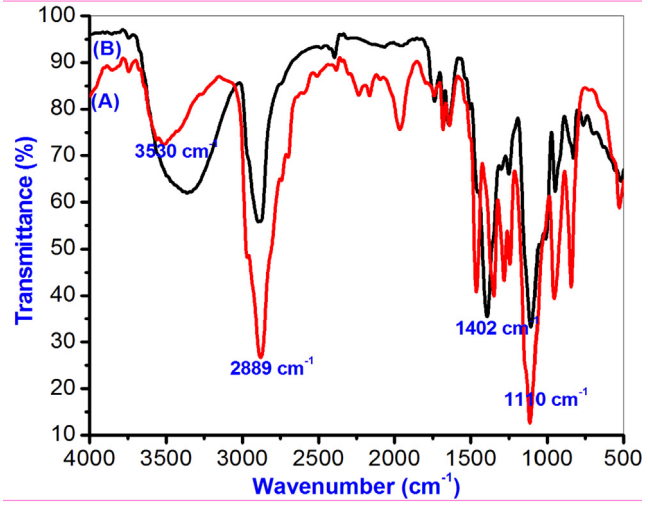

Figure 1 Fourier transform infrared spectroscopic (FTIR) studies of as prepared $AgNO_3$/F127 composite gel carried out before calcination. (A) pure Pluronic F127, (B) $AgNO_3$/F127 composite gel.

1. Introduction

Metallic porous materials are of great interest for heterogeneous catalysis, sensor technology, electrochemical supercapacitors, fuel cell electrodes, bio-filtration capability, medicine, photonic crystals, chemical separations, and photocatalysis [1–8]. Among these metallic porous materials, silver is the dynamic and highly efficient promising material for various biomedical applications because of its environmentally benign and eco-friendly nature [9–17]. The non-toxicity and bactericidal activity of silver materials makes it an efficient choice for multiple roles in the medical field including in the formulation of dental resin composites; as a bactericidal coating in water filters; as an antimicrobial agent in air sanitizer sprays, in coatings of medical devices; detergents, socks, wet wipes, toothpastes, soaps, shampoos, pillows, respirators, washing machines, and many other consumer products; as bone cement; and in many wound dressings to name a few [9–17].

There are many synthetic routes that have been explored to fabricate porous silver based materials for many bio-medical applications [18,19]. Among the synthetic routes include: electrochemical [20], sonochemical [21], sol–gel [22–24], microwave [25], radiation assisted process [26], photochemical [27] and currently by green chemistry synthesis [28,29]. Although porous noble metal materials have been used extensively in these potential applications still the synthesis of hierarchical porous noble metal materials is challenging despite significant progress in preparing micro-meso and macrostructured porous materials of metal and metal oxides.

Here, we have synthesized hierarchically macroporous silver monoliths using Pluronic F127 as a reducing agent via modified sol gel route without using any acidic or basic medium i.e. "green" approach and the most significant advantage of the reported method is that conditions of high temperature, pressure, and toxic chemicals are not required in the synthesis protocol. Furthermore, we examined the bactericidal activity of as synthesized metallic porous silver monoliths against Gram negative and Gram positive pathogens (*Escherichia coli*, *Salmonella typhimurium* and *Bacillus subtilis*), comparing its properties with that of standard antibiotic (amoxicillin) by using Kirby–Bauer disk diffusion method.

2. Experimental

2.1. Synthesis of macroporous metallic silver monoliths

In a typical synthesis, 2.0 g of silver nitrate (50 wt.%, BDH) in 2.0 g of ultrapure water (50 wt.%) was added to 2.0 g of soft template Pluronic F127 (polyethylene oxide – polypropylene oxide – polyethylene oxide, $[(EO)_{106}\ (PO)_{70}\ (EO)_{106}]$, 14.81 wt.%, Aldrich) in 11.50 g of ultrapure water (85.19 wt.%) and stirred vigorously. The gel was stirred at room temperature for 1 h to form the paste which gradually became dark in color. The resulting gel was aged for 48 h at room temperature

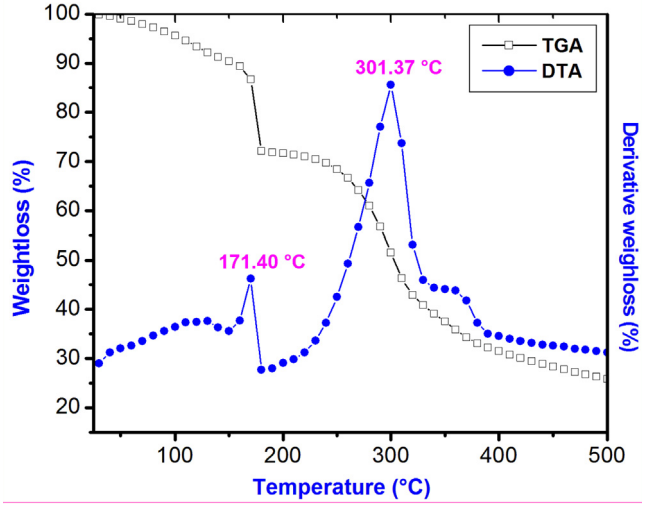

Figure 2 TGA-DTA profile of $AgNO_3$/F127 composite gel.

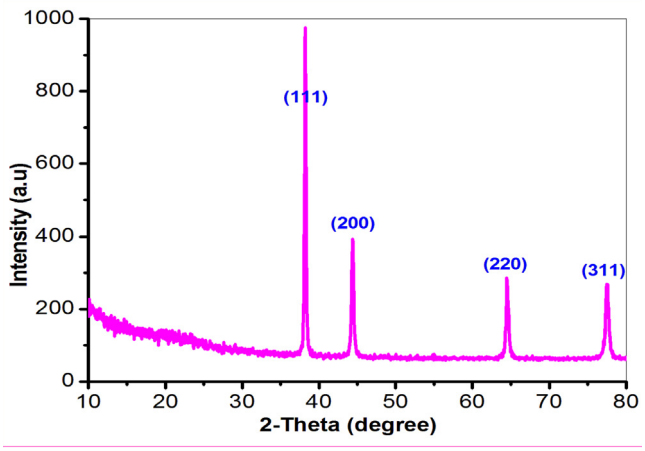

Figure 3 XRD patterns of macroporous silver particles prepared by using F127 as a reducing agent obtained after the calcination of $AgNO_3$/F127 composite gel.

and then calcined at 650 °C for 2 h at a heating rate of 2 °C/min followed by cooling at a rate of 2 °C/min to room temperature in an ELLITE furnace.

2.2. Structural characterization

The mode of cross linking of precursor silver nitrate ($AgNO_3$) with soft template Pluronic F127 ($AgNO_3$/F127 gel) was analyzed by Shimadzu-8400S spectrometer. Perkin-Elmer thermal analyzer was used for Thermogravimetric (TG) analysis using alumina reference crucible at the heating rate of 10 °C/min. Crystal structure of the calcined silver monoliths was confirmed by Bruker D-8 advance diffractometer in the diffraction angle range 2θ = 10–90°, using monochromatic Cu kα radiations (λ = 1.5401 Å). The surface pore morphology and average pore diameter of the obtained sample was carried out by field emission scanning electron microscopy (FESEM) using NOVA NANOSEM 450 microscope equipped to perform elemental chemical analysis by energy dispersive X-ray spectroscopy (EDX). BET specific surface area and pore volume of the calcined porous silver materials was estimated by physisorption of N_2 at 77 K over a Micromeritics ASAP 2010.

2.3. Microorganisms and medium

The strains of pathogens such as *E. coli* (MTCC 40, Gram negative), *S. typhimurium* (MTCC 98, Gram negative) and *B. subtilis* (MTCC 619, Gram positive) used for the antibacterial activity were obtained from the Institute of Microbial Technology (IMTECH), Chandigarh, India and conserved in the laboratory. Muller–Hinton (MH) agar medium used for this study contains the following: 2 g beef infusion, 1.5 g soluble starch, 17.5 casein hydrolysate, 20 g Agar–Agar, 1 g distilled water, and pH 7.2 ± 0.3.

2.4. Antibacterial activity assessment

The antimicrobial activity of as synthesized macroporous metallic silver monoliths was tested against three strains of pathogens (*E. coli* (MTCC 40), *S. typhimurium* (MTCC 98), and *B. subtilis* (MTCC 619)) using disk-diffusion method. Overlays of each test strain (10^6 CFU/ml) were prepared on Muller Hinton agar plates and allowed to dry. Paper disks (5 mm) were cut and impregnated in solutions of different concentrations of 50 μg ml^{-1}, 100 μg ml^{-1} and 150 μg ml^{-1} of macroporous silver monoliths for 5 min and subsequently allowed to dry under sterile conditions. The dried paper disks were kept in the agar plates and incubated for 24 h. The standard antibiotic amoxicillin (100 μg ml^{-1}) was used as a positive control. The diameter of zone of inhibition after incubation at 37 °C/24 h was measured and the experiments were done in triplicates and finally the mean results are represented.

3. Results and discussion

3.1. FTIR study of the ($AgNO_3$/F127) composite gel

The complexation of biocompatible non ionic surfactant Pluronic F127 with the $AgNO_3$ precursor was examined before calcination by FTIR (Fig. 1). Comparing the FTIR spectrum of Pure surfactant Pluronic F127 with the FTIR spectrum of composite gel ($AgNO_3$-F127), it was found that there is a shift in peaks from 3530 cm^{-1}, 2889 cm^{-1}, 1402 cm^{-1} and 1110 cm^{-1} corresponding to asymmetric stretching vibrations of —O—H, —C—H, —C—C and —C—O of pure surfactant Pluronic F127 (EO_{106} PO_{70} EO_{106}) to lower wavenumber which is attributed to the cross linking of Ag^+ cations with hydrophilic part of the surfactant [EO] by a combination of electrostatic and van der Waals interactions and formed ordered matrix [30]. This method is a promising alternative "green" approach for the synthesis of micro-meso and

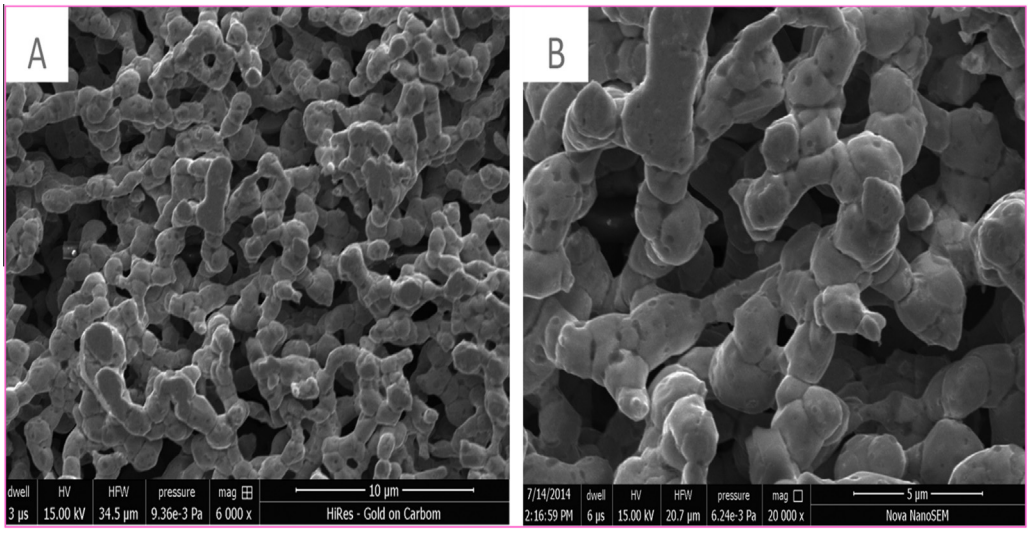

Figure 4 FESEM micrographs of macroporous silver monoliths synthesized using F127 as a non-ionic surfactant obtained after the calcination of $AgNO_3$/F127 composite gel. (A) Panoramic SEM image with a hierarchical network of pores (average pore diameter 600 nm), scale bar = 10 μm, (B) showing interconnected pores ranging from 100 to 350 nm, scale bar = 5 μm.

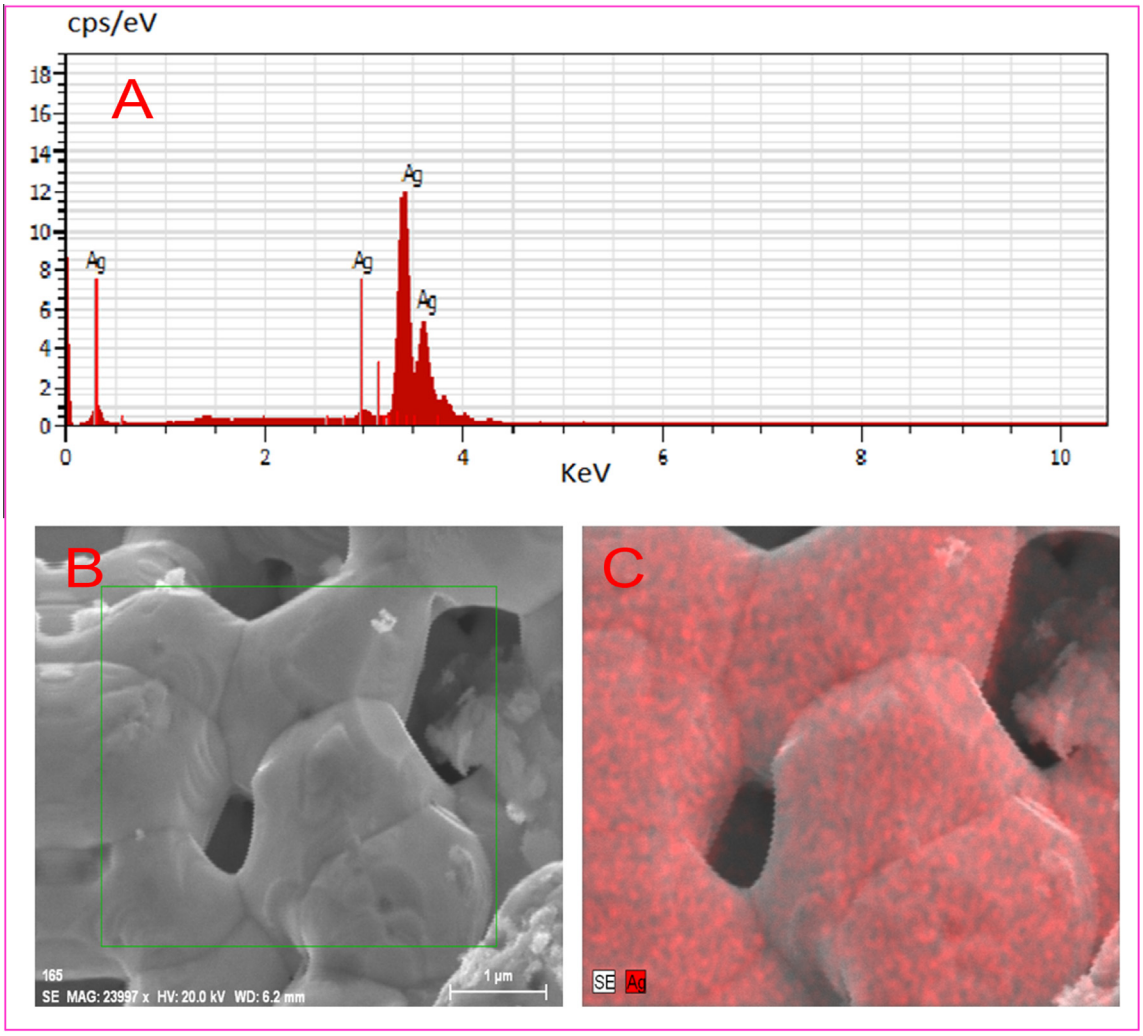

Figure 5 EDX elemental and mapping analysis of macroporous (MP) silver monoliths (A) elemental composition analysis, (B) the portion of FESEM image used for the mapping (C) EDX mapping data carried out for 15 min where red spots showing presence of silver particles.

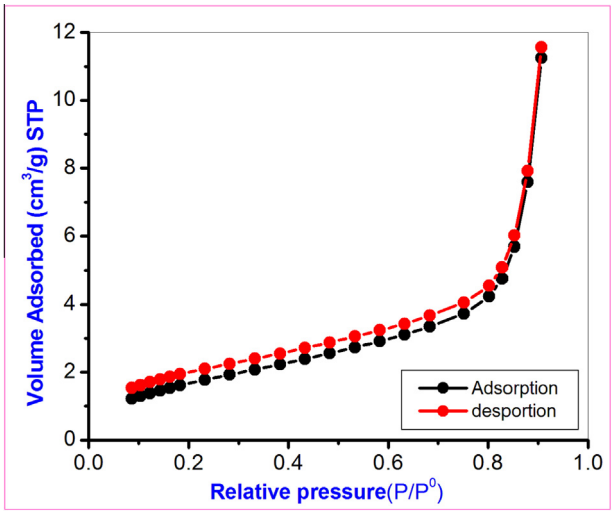

Figure 6 N_2 sorption isotherms for macroporous silver monoliths obtained after the calcination of $AgNO_3$/F127 composite gel.

macrostructured porous materials while avoiding the need of acidic or basic medium.

3.2. TGA-DTA studies of the (AgNO₃/F127) composite gel

The TG-DTA profile of the as synthesized ($AgNO_3$/F127) composite gel (sample weight taken = 13.0230 mg) was carried out before calcination. Fig. 2 shows an initial weight loss of 4.320% (0.5627 mg) up to 165 °C due to the removal of physically absorbed water followed by 29.10% (3.789 mg) weight loss at 165–210 °C associated with thermal transformation of silver nitrate to silver nitrite, O_2 and NO_2 [22]. The concomitant release of O_2 facilitated oxidative decomposition of Pluronic F127 between 210 and 430 °C with a considerable mass loss of 35.21% (4.585 mg). The residual silver materials left are of 31.37 weight% (4.0863 mg). In DTA profile, the two exothermic peaks obtained at ca. 171.40 °C and 301.37 °C are corresponding to the decomposition of soft template Pluronic F127 and the combustion of remaining carbon species [30] respectively.

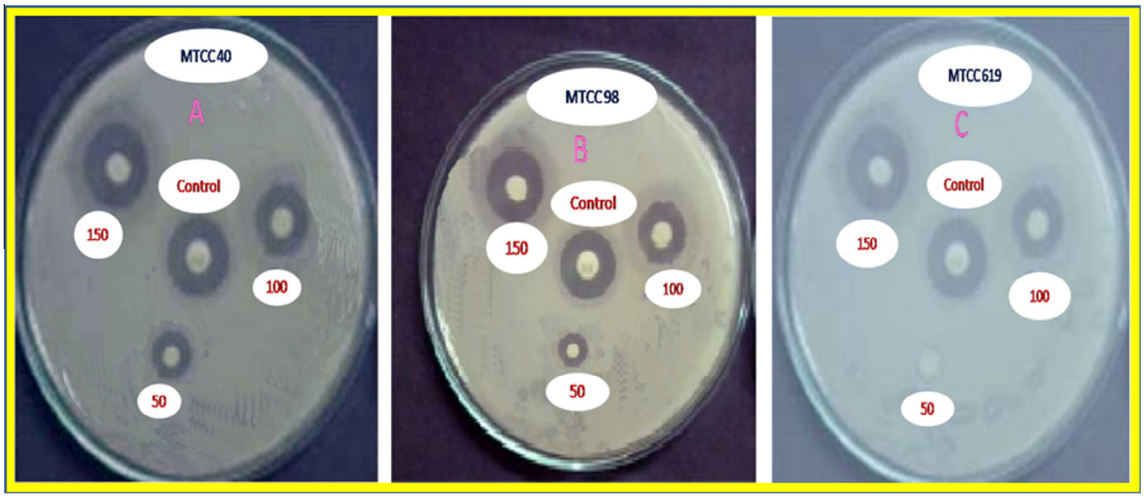

Figure 7 Zone of inhibition of macroporous (MP) silver monoliths against three pathogens: (A) *E. coli* (MTCC 40), (B) *S. typhimurium* (MTCC 98), (C) *B. subtilis* (MTCC 619).

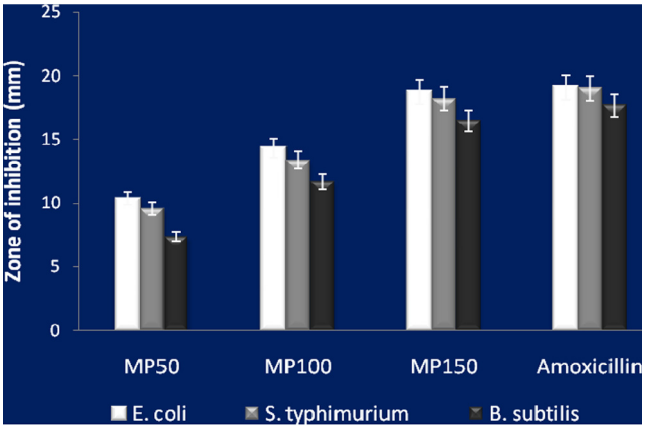

Figure 8 Graphical representation of growth inhibition of different concentration of macroporous (MP) silver monoliths (50 μg ml^{-1}, 100 μg ml^{-1}, 150 μg ml^{-1}) and positive control amoxicillin (100 μg ml^{-1}) in *E. coli* (MTCC 40), *S. typhimurium* (MTCC 98), *B. subtilis* (MTCC 619).

3.3. X-ray diffraction analysis

The crystalline structure and phase purity of the as-synthesized sample was examined by XRD (Fig. 3). All the peaks with d spacings of 2.35, 2.04, 1.44, and 1.23 Å corresponding to (1 1 1), (2 0 0), (2 2 0), and (3 1 1) lattice planes of a face centered cubic unit cell (JCPDS File No. 04-0783) associated with m3m point group and Fm3m/225 space group symmetry [28,31–33]. No characteristic peaks of any impurity were detected, suggesting that high quality porous metallic silver monoliths were prepared.

3.4. FESEM-EDX analysis

The synthesized macroporous silver monoliths were characterized by FESEM and EDX studies. FESEM studies revealed a continuous interconnected scaffold with a hierarchical network of pores with an average pore diameter of 600 nm (Fig. 4A). A close inspection of the Fig. 4(A) admits that the interparticle pore size on the walls is in the range of 30–45 nm. The disordered network of macroporous voids are likely to be formed by the reduction of the silver ions by hydroxyl group (—OH) of non ionic surfactant Pluronic F127 which are removed by calcination. We also encounter regions of smooth silver frameworks with interconnected pores of a few hundred nanometers ranging from 100 to 350 nm (Fig 4B). The final macroporous silver monoliths can form a perfect integrated network of structure with a well developed electron conductive network and efficient release of silver ions for killing the bacterial cell. Moreover, the purity of macroporous silver particles was further confirmed by EDX elemental and mapping studies (Fig 5A–C). Fig 5(A) indicates the macroporous silver is nearly stoichiometric (100 wt.%), obtained from EDX elemental analysis results. The EDX mapping results of macroporous silver particles obtained supported the fabrication of pure silver matrix (Fig. 5B and C). Thus the EDX elemental and mapping results verify that the as-synthesized sample is purely composed of Ag.

3.5. BET surface area analysis of macroporous silver monoliths

Fig. 6 displays the nitrogen sorption isotherms performed on a 120 mg sample. The adsorption/desorption curve is characterized by a hysteresis loop associated with capillary condensation at a high relative pressure (>0.8). The curve corresponds to the Type II isotherms according to the IUPAC classification featuring the macroporous characteristics of the porous metallic silver particles [34] associated with BET specific surface area of 20 m^2/g and pore volume 0.04703 (cm^3/g) with respect to gas adsorption in macropores (widths > 50 nm) [34]. The initial part (low relative pressures) of the isotherms in Fig. 6 reveals the monolayer adsorption; the quantity of nitrogen gas adsorbed in that range is used by BET surface area analyzer instrument (Micromeritics ASAP 2010) for the evaluation of specific surface area according to the BET method.

4. Antibacterial activity of macroporous silver monoliths

Silver nanoparticles were found to be best biocide, for example in wound dressings and as an antimicrobial coating on consumer products but the major problems such as aggregation, agglomeration, oxidation and inactivation of silver nanoparticles, numerous preventive measures have been employed. To overcome these issues fabrication and application of porous silver monoliths as biomaterials are currently in great interest because of their good stability, three-dimensional porosity, high aspect ratio, good surface to volume ration, high number of active sites, highly active surface silver atoms, efficient bactericidal activity, good materials for bio-separations, drug delivery and importance in biomedical devices [1–10].

In this study, macroporous silver monoliths were tested against two strains of Gram negative pathogens (*E. coli*, MTCC 40, *S. typhimurium*, MTCC 98), and a Gram positive pathogen (*B. subtilis*, MTCC 619) using disk-diffusion method. It has been observed that the presence of macroporous (MP) silver at a concentration of 50 μg ml^{-1} against all three pathogens have shown little zone of inhibition while as marked zone of inhibition was found at concentration of 150 μg ml^{-1} (Fig. 7). The results indicate that at moderate concentration (150 μg ml^{-1}) of MP silver monoliths have excellent antibacterial properties. Moreover, in the deep study of antibacterial property of MP silver monoliths against the mentioned pathogens, incredible results have been obtained against *E. coli* (MTCC 40) which might be attributed to the strong interaction of released silver ions from the MP silver source with the cell wall composition of *E. coli* (Fig. 8). As compared to the standard antibiotic amoxicillin (100 μg ml^{-1}), the MP silver monoliths have shown effective antibacterial effects against the Gram negative pathogens (*E. coli* and *S. Typhimurium*) while as moderate antibacterial effect against Gram positive pathogen (*B. subtilis*) which might be attributed to the different membrane structures of Gram-positive and Gram-negative bacteria [35].

The cell wall of Gram negative bacteria possesses an outer membrane of lipopolysaccharide followed by a 2–3 nm thin peptidoglycan layer while Gram-positive bacteria lack the outer membrane but have a thick (about 30 nm) layer of peptidoglycan, consisting of linear polysaccharide chains cross-linked by short peptides to form a three dimensional rigid structure which provides very few anchoring sites for nanoporous silver materials in the cell wall thus leading to difficulty in penetration [36]. Another reason of good bactericidal effects of porous silver materials with Gram negative bacteria may be attributed to better electrostatic interaction between positive charges of released silver ions from porous silver monoliths with abundant negative charges of lipopolysaccharide of Gram-negative bacteria than Gram-positive bacteria [36]. Enhanced bactericidal effects of porous silver monoliths may

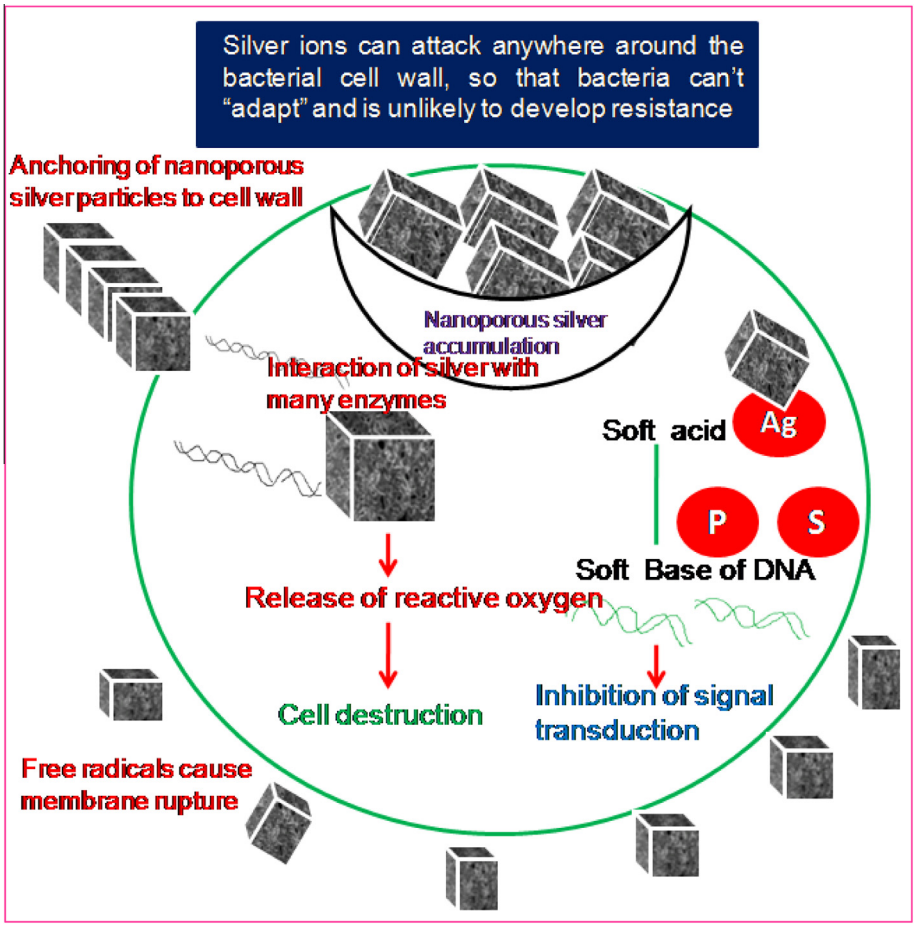

Figure 9 Plausible mechanisms of bactericidal effects of porous silver materials.

be also attributed to spaces among the porous materials which are providing access for the bacteria to enter and the protruding ligaments are attached to the membranes to damage the bacteria [9].

4.1. Plausible mechanisms of antibacterial effects of macroporous silver materials

The absolute mechanism of antibacterial action of silver materials is not sharp or clear and still remained a topic of discussion. However, there are various theories with solid mechanisms on the action of silver materials to cause biocidal effect. Ag^+ ions released from the porous silver monoliths when coming in close contact of bacterial cell wall leading to the structural changes like the permeability of the cell membrane and thus death of the cell. The accumulation and aggregation of Ag^+ ions released from the porous silver materials on the cell surface resulting in the formation of free radicals, having the ability to damage the cell membrane and ultimately leading to cell death, may be considered another mechanism of biocidal effect of silver materials [40–42]. It has been proposed that interaction of silver ions with the thiol group of many vital enzymes or proteins (DNA) leading to enhanced pyrimidine dimerization by photodynamic reaction and possible prevention of DNA replication because of highly stable interaction of soft acid Ag^+ with the soft bases (P and S) of DNA, damages the bacterial structure and thus leading to the death of bacteria. Scientists have also proved that during antibacterial activity of silver materials, oxygen associates with silver ions released from the silver source materials and reacts with the sulfhydryl (—S—H) groups on cell wall to form R—S—S—R bonds thus, blocking respiration and causing death of cells [35–39,40–42] (Fig. 9).

5. Conclusion

An efficient synthetic approach for the fabrication of macroporous silver monoliths have been explored which can ‘‘switch off” other existing methods because of its ability for concise tuning of porous materials by changing surfactants and using different structural directing agents in the synthesis protocol. The as-synthesized macroporous silver monoliths have proved to be essential candidates for the antibacterial activity. It has been concluded that antibacterial property of porous metal and metal oxide materials can be more enhanced by concise tuning of surface pore size morphology. We believe that the development of the eco-friendly and non-toxic antibacterial agents such as metal and metal oxide porous materials will serve as an alternative to traditional antibiotics and might be promising for the future of pharmaceutics and medicine.

Acknowledgement

GAN and MUDS acknowledge UGC New Delhi for financial assistance through Central University Fellowship (CUF) and MT acknowledges UGC for Rajiv Gandhi National Fellowship (RGNF). MAG is thankful to National Council for Scientific and Technological Development, Brazil for providing Post doctorate fellowship (Science without Border) and Department of Zoology, Dr. Hari Singh Gour University, Sagar, for antibacterial activities. Authors also acknowledge Head, Department of Chemistry, and Sophisticated Instrument Centre (SIC) Dr. Hari Singh Gour Central University, Sagar, for providing the necessary facilities to carry out this research work.

References

[1] G.A. Naikoo, R.A. Dar, F. Khan, Hierarchically macro/mesostructured porous copper oxide: facile synthesis, characterization, catalytic performance and electrochemical study of mesoporous copper oxide monoliths, J. Mater. Chem. A 2 (2014) 11792–11798.
[2] R.A. Dar, G.A. Naikoo, P.K. Kalambate, L. Giri, F. Khan, S.P. Karna, A.K. Srivastava, Enhancement of the energy storage properties of supercapacitors using graphene nanosheets dispersed with macro-structured porous copper oxide, Electrochem. Acta 163 (2015) 196–203.
[3] F.Q. Sun, W.P. Cai, Y. Li, L.C. Jia, F. Lu, Direct growth of mono- and multilayer nanostructured porous films on curved surfaces and their application as gas sensor, Adv. Mater. 17 (2005) 2872.
[4] B.Y. Xia, W.T. Ng, H.B. Wu, X. Wang, X.W. Lou, Self-supported interconnected Pt nano-assemblies as highly stable electrocatalysts for low-temperature fuel cells, Angew. Chem. Int. Ed. 51 (2012) 7213.
[5] L. Zhou, D.Y. Zhao, X.W. Lou, Hollow structures as high-performance cathodes for lithium-ion batteries, Angew. Chem. Int. Ed. 51 (2012) 239.
[6] Y. Liu, H. Dai, J. Deng, L. Zhang, C.T. Au, Three-dimensional ordered macroporous bismuth vanadates: PMMA-templating fabrication and excellent visible light-driven photocatalytic performance for phenol degradation, Nanoscale 4 (2012) 2317–2325.
[7] Y. Wei, J. Liu, Z. Zhao, A. Duan, G. Jiang, C. Xu, J. Gao, H. He, X. Wang, Three-dimensionally ordered macroporous $Ce_{0.8}Zr_{0.2}O_2$-supported gold nanoparticles: synthesis with controllable size and super-catalytic performance for soot oxidation, Energy Environ. Sci. 4 (2011) 2959–2970.
[8] Y. Wei, J. Liu, Z. Zhao, A. Duan, G. Jiang, The catalysts of three-dimensionally ordered macroporous $Ce_{1-x}Zr_xO_2$-supported gold nanoparticles for soot combustion: the metal–support interaction, J. Catal. 287 (2012) 13–29.
[9] I. Sondi, B. Salopek-Sondi, Silver nanoparticles as antimicrobial agent: a case study on *E. coli* as a model for Gram-negative bacteria, J. Colloid Interface Sci. 275 (2004) 177.
[10] A. Melaiye, Z. Sun, K. Hindi, A. Milsted, D. Ely, D.H. Reneker, C.A. Tessier, W.J. Youngs, Silver (I)-imidazole cyclophane gem-diol complexes encapsulated by electrospun tecophilic nanofibers: formation of nanosilver particles and antimicrobial activity, J. Am. Chem. Soc. 127 (2005) 2285.
[11] K.J. Kim, W.S. Sung, B.K. Suh, S.K. Moon, J.S. Choi, J.G. Kim, D.G. Lee, Antifungal activity and mode of action of silver nanoparticles on Candida albicans, Biometals 22 (2009) 235–242.
[12] P.E. Petrochenko, S.A. Skoog, Q. Zhang, D.J. Comstock, J.W. Elam, P.L. Goering, R.J. Narayan, Cytotoxicity of cultured macrophages exposed to antimicrobial zinc oxide (ZnO) coatings on nanoporous aluminum oxide membranes, Biomatter (2013), doi: e25528-1–e25528-7.
[13] I. Subhankari, P.L. Nayak, Antimicrobial activity of copper nanoparticles synthesised by ginger (*Zingiber officinale*) extract, World J. Nano Sci. Technol. 2 (2013) 10–13.
[14] K.B. Holt, A.J. Bard, Interaction of silver (I) ions with the respiratory chain of *Escherichia coli*: an electrochemical and scanning electrochemical microscopy study of the antimicrobial mechanism of micromolar Ag+, Biochemistry 44 (2005) 13214–13223.

[15] C. Aymonier, U. Schlotterbeck, L. Antonietti, P. Zacharias, R. Thomann, J.C. Tiller, S. Mecking, Hybrids of silver nanoparticles with amphiphilic hyperbranched macromolecules exhibiting antimicrobial properties, Chem. Commun. 24 (2002) 3018–3019.
[16] V. Alt, T. Bechert, P. Steinrucke, M. Wagener, P. Seidel, E. Dingeldein, E. Domann, R. Schnettler, An in vitro assessment of the antibacterial properties and cytotoxicity of nanoparticulate silver bone cement, Biomaterials 25 (2004) 4383–4391.
[17] V. Thomas, M.M. Yallapu, B. Sreedhar, S.K. Bajpai, A versatile strategy to fabricate hydrogel–silver nanocomposites and investigation of their antimicrobial activity, J. Colloid Interface Sci. 315 (2007) 389–395.
[18] S. Pal, Y.K. Tak, J.M. Song, Does the antibacterial activity of silver nanoparticles depend on the shape of the nanoparticle? a study of the gram-negative bacterium *Escherichia coli*, Appl. Environ. Microbiol. 73 (2007) 1712.
[19] G.A. Martinez-Castanon, N. NinoMartinez, F. Martinez-Gutierrez, J.R. Martinez-Mendoza, F. Ruiz, Synthesis and antibacterial activity of silver nanoparticles with different sizes, J. Nanopart. Res. 10 (2008) 1343–1348.
[20] L. Rodriguez-Sanchez, M.C. Blanco, M.A. Lopez-Quintela, Electrochemical synthesis of silver nanoparticles, J. Phys. Chem. B 104 (2000) 9683–9688.
[21] I. Perelshtein, G. Applerot, N. Perkas, G. Guibert, S. Mikhailov, A. Gedanken, Sonochemical coating of silver nanoparticles on textile fabrics (nylon, polyester and cotton) and their antibacterial activity, Nanotechnology 19 (2008) 245705.
[22] F. Khan, S. Mann, Fabrication of metal and metal oxide sponges by self-bubbled triton X-45 hydrogel templates, J. Phys. Chem. C 113 (2009) 19871–19874.
[23] D. Walsh, I. Arceli, T. Ikoma, S. Tanaka, S. Mann, Dextran templating for the synthesis of metallic and metal oxide sponges, Nat. Mater. 2 (2003) 386–390.
[24] F. Khan, M. Eswaramoorthy, C.N.R. Rao, Macroporous silver monoliths using a simple surfactant, Solid State Sci. 9 (2007) 27–31.
[25] H. Yin, T. Yamamoto, Y. Wada, S. Yanagida, Large-scale and size-controlled synthesis of silver nanoparticles under microwave irradiation, Mater. Chem. Phys. 83 (2004) 66–70.
[26] K. Shameli, M.B. Ahmad, W.M.Z.W. Yunus, N.A. Ibrahim, Y. Gharayebi, S. Sedaghat, Synthesis of silver/montmorillonite nanocomposite using γ-irradiation, Int. J. Nanomed. 5 (2010) 1067–1077.
[27] K. Mallick, M.J. Witcomb, M.S. Scurrell, Polymer stabilized silver nanoparticles: a photochemical synthesis route, J. Mater. Sci. 39 (2004) 4459–4463.
[28] K. Shameli, M. Ahmad, W.M.Z.W. Yunus, A. Rustaiyan, N.A. Ibrahim, M. Zargar, Y. Abdollahi, Green synthesis of silver/montmorillonite/chitosan bionanocomposites using the UV irradiation method and evaluation of antibacterial activity, Int. J. Nanomed. 5 (2010) 875–887.
[29] P. Raveendran, J. Fu, S.L. Wallen, Completely "green" synthesis and stabilization of metal nanoparticles, J. Am. Chem. Soc. 125 (2003) 13940–13941.
[30] H. Zhang, C. Tang, Y. Lv, C. Sun, F. Gao, L. Dong, Y. Chen, Synthesis, characterization, and catalytic performance of copper-containing SBA-15 in the phenol hydroxylation, J. Colloid Interface Sci. 380 (2012) 16–24.
[31] B.D. Cullity, Elements of X-ray Diffraction, Addison-Wesley Company, USA, 1956.
[32] R. John, S.S. Florence, Structural and optical properties of ZnS nanoparticles synthesized by solid state reaction method, Chalcogenide Lett. 6 (2009) 535–539.
[33] A.M. Theivasanthi, M. Alagar, X-ray diffraction studies of copper nanopowder, Arch. Phys. Res. 1 (2010) 112–117.
[34] J. Yan, T. Wei, Z. Fan, W. Qian, M. Zhang, X. Shen, F. Wei, Preparation of graphenenanosheet/carbon nanotube/polyaniline composite as electrode material for supercapacitors, J. Power Sources 195 (2010) 3041–3045.
[35] C. Zhang, X. Wang, J. Sun, T. Koua, Z. Zhang, Synthesis and antibacterial properties of magnetically recyclable nanoporous silver/Fe3O4 nanocomposites through one-step dealloying, Cryst. Eng. Commun. 15 (2013) 3965–3973.
[36] M. Banerjee, S.A. Sharma, Chattopadhyay, S.S. Ghosh, Enhanced antibacterial activity of bimetallic gold-silver core–shell nanoparticles at low silver concentration, Nanoscale 3 (2011) 5120–5125.
[37] M. Danilcauk, A. Lund, J. Saldo, H. Yamada, J. Michalik, Conduction electron spin resonance of small silver particles, Spectrochim. Acta A 63 (2006) 189–191.
[38] J.S. Kim, E. Kuk, K. Yu, J.H. Kim, S.J. Park, H.J. Lee, et al, Antimicrobial effects of silver nanoparticles, Nanomedicine 3 (2007) 95–101.
[39] J.R. Morones, J.L. Elechiguerra, A. Camacho, K. Holt, J.B. Kouri, J.T. Ramirez, M.J. Yacaman, The bactericidal effect of silver nanoparticles, Nanotechnology 16 (2005) 2346–2353.
[40] S. Shrivastava, T. Bera, A. Roy, G. Singh, P. Ramachandrarao, D. Dash, Characterisation of enhanced antibacterial effects of novel silver nanoparticles, Nanotechnology 18 (2007) 1–9.
[41] K. Cho, J. Park, T. Osaka, S. Park, The study of antimicrobial activity and preservative effects of nanosilver ingredient, Electrochem. Acta 51 (2005) 956–960.
[42] V.S. Kumar, B.M. Nagaraja, V. Shashikala, A.H. Padmasri, S. S. Madhavendra, B.D. Raju, Highly efficient Ag/C catalyst prepared by electro-chemical deposition method in controlling microorganisms in water, J. Mol. Catal. A Chem. 223 (2004) 313–319.